THE JOURNAL OF BIOLOGICAL CHEMISTRY

Vol. 260, No. 17, Issue of August 15, pp. 9537-9544, 1985
Printed in U.S.A.

Evidence that Anion Transport by Band 3 Proceeds via a Ping-Pong Mechanism Involving a Single Transport Site

A ^{35}Cl NMR STUDY*

(Received for publication, August 20, 1984)

Joseph J. Falke and Sunney I. Chan‡

From the Arthur Amos Noyes Laboratory of Chemical Physics, California Institute of Technology, Pasadena, California 91125

Band 3 catalyzes the one-for-one exchange of monovalent anions across the red cell membrane. At least two anion binding sites have been postulated to exist on the transport unit: 1) a transport site that has been observed by saturation kinetics and by ^{35}Cl NMR studies of chloride binding, and 2) a ^{35}Cl NMR-invisible inhibitory site that has been proposed to explain the inhibition of anion exchange at large anion concentrations. A number of independent studies have indicated that the transport site is alternately exposed to different sides of the membrane during the transport cycle. Yet the role, if any, of the postulated inhibitory site in the transport cycle is not known. Here it is shown that: 1) when the $[Cl^-]$, $[Br^-]$, or pH is varied, the band 3 transport sites on both sides of the membrane behave like a homogeneous population of simple anion binding sites in ^{35}Cl NMR experiments, and 2) when the $[Cl^-]$ is varied, the outward-facing transport site behaves like a simple anion binding site. These results indicate that the postulated inhibitory site has no effect on chloride binding to the transport site. Instead, the results are quantitatively consistent with the ping-pong model (Gunn, R. B., and Frölich, O. (1979) *J. Gen. Physiol.* 74, 351–374), which states that the transport site is the *only* site involved in the transport cycle. Expressions are derived for the macroscopically observed characteristics of a ping-pong transporter: these characteristics are shown to be weighted averages of the microscopic properties of the inward- and outward-facing conformations of the transport site.

In addition to supporting the simplicity of the transport mechanism, the high pH titration curve for chloride binding to the transport site provides insight into the structure of the site. The macroscopically observed $pK_A = 11.1 \pm 0.1$ in the leaky ghost system indicates that an arginine must provide the essential positive charge in the inward- or outward-facing conformation of the transport site, or in both conformations.

Band 3 is a 95,000-dalton transmembrane protein that catalyzes the one-for-one exchange of two monovalent anions in opposite directions across the membrane of the human red cell. The physiological substrate anions of this protein are bicarbonate, produced by the hydration of carbon dioxide and chloride. The passive exchange of these anions by band 3 is essential to the respiration of carbon dioxide; as a result, the band 3 anion transport system is the most heavily used ion transport pathway in typical vertebrate organisms (1, 2).

We have been interested in obtaining a molecular picture of the ion transport event in band 3. A first step in the development of such a picture is the determination of the chemical and kinetic equations that describe the transport cycle; the present paper focuses on the chemical equation. Some features of the transport cycle have already been established. One of the key findings is that band 3 is an alternating site transporter possessing a single transport site that is alternately exposed to opposite sides of the membrane. This site can only cross the membrane when it is occupied by substrate anion; thus, when a chloride gradient is imposed across the membrane, the transport site accumulates on the side of the membrane exposed to low chloride concentration (3). Recently, ^{35}Cl NMR has been used to resolve band 3 transport sites on opposite sides of the membrane. Such experiments have confirmed the alternating site mechanism; the inhibitor 4,4′-dinitrostilbene-2,2′-disulfonate (DNDS[1]), which binds exclusively to the outward-facing transport site, was observed to recruit the transport site exclusively to the outward-facing conformation (4).

Although there now exists a substantial body of evidence indicating that band 3 possesses a single, alternating transport site, it is not yet possible to exclude the existence of other anion binding sites on the protein which do not transport anions but which may be involved in the transport cycle. For example, one or more inhibitory anion binding sites have been postulated to explain the inhibition of band 3 catalyzed anion exchange that is observed at sufficiently large anion concentrations (5–7). Thus, it is important to determine whether the transport cycle involves only the transport site or other sites as well. The simplest form of the alternating site mechanism, termed the ping-pong mechanism by Gunn and Frölich (8), proposes that the transport site is in fact the only site involved in the normal transport cycle.

The ping-pong model makes a set of predictions that are amenable to quantitative tests when ^{35}Cl NMR is used to observe transport site behavior. These predictions involve the heterogeneity of the inward- and outward-facing transport sites. A variety of existing evidence is consistent with the idea that the two transport site orientations are structurally different: 1) substrate ions such as Cl^- and Br^- exhibit greater apparent affinities for the outward-facing sites than for inward-facing sites in transport saturation experiments (8), although such differences could be due to differences in translocation rate constants as well as differences in site structure (9), and 2) organo-anions that competitively inhibit substrate binding to the transport sites generally bind more tightly to

* This work was supported by National Institute of General Medical Sciences Grant GM-22432 (to S.I.C.) and by a National Science Foundation predoctoral fellowship (to J.J.F.). Contribution 7068 from the Arthur Amos Noyes Laboratory of Chemical Physics. The costs of publication of this article were defrayed in part by the payment of page charges. This article must therefore be hereby marked "*advertisement*" in accordance with 18 U.S.C. Section 1734 solely to indicate this fact.

‡ To whom reprint requests should be sent.

[1] The abbreviation used is: DNDS, 4,4′-dinitrostilbene-2,2′-disulfonate.

the extracellular face of the protein, where they occupy the outward-facing transport site (9). Despite this evidence, which indicates that the structure of the transport site and/or its surroundings must change upon translocation, the ping-pong model predicts that the inward- and outward-facing transport sites will together behave like a homogeneous population of transport sites in macroscopic experiments. In the present paper we introduce ^{35}Cl NMR data indicating that when the $[Cl^-]$, $[Br^-]$, or pH is varied, the inward- and outward-facing band 3 transport sites exhibit the macroscopic homogeneity required by the ping-pong model. In short, the results are completely consistent with a transport cycle in which the transport site is the only important site. The kinetic equation for this transport cycle is the subject of the following companion paper (10).

MATERIALS AND METHODS

All chemicals used were reagent grade or better; packed red cells were the kind gift of the Los Angeles Chapter of the American Red Cross.

All of the following procedures were carried out exactly as previously described in detail (2, 4). Leaky red cell ghost membranes (2) were prepared by osmotic lysis of intact red cells, followed by extensive washing to remove the cytoplasmic contents of the cells. The isolated membranes were stored at 4 °C for no more than 4 days in 5 mM NaH_2PO_4, pH to 8 with NaOH, 130 μM dithiothreitol, and 10 μM phenylmethylsulfonyl fluoride. Where appropriate, crushed ghosts (4) or sonicated ghosts (4) were made from leaky ghosts. NMR samples were made on ice by diluting the isolated membranes with an equal volume of ice cold 2 × NMR buffer and were assayed by ^{35}Cl NMR the same day. The $^{35}Cl^-$ line broadening due to band 3 transport sites was isolated from the line broadening due to other sites using DNDS, a competitive inhibitor of chloride binding to band 3 transport sites; subtraction of the line broadening of a membrane sample containing 1 mM DNDS from the line broadening of an identical sample lacking DNDS yielded the transport site line broadening. All line broadenings were normalized to the same band 3 concentration by dividing each sample by its total ghost protein concentration, determined by Lowry protein analysis (11, 12).

The pH titration samples were prepared by incrementally adding 2 N NaOH or HCl to a sufficiently large volume of sonicated ghost membranes in NMR buffer on ice. When the pH reached a desired value, two aliquots were removed. DNDS in H_2O was added to one of the samples, and the same volume of H_2O to the other. This enabled determination of the transport site line broadening at the desired pH as described above and, in complete detail, previously (2, 4). The samples that resulted were virtually identical except with respect to pH and DNDS concentration, since the added acid or base only negligibly altered the chloride concentration and the sample volume.

RESULTS

The ^{35}Cl NMR Assay—The work presented here examines the characteristics and mechanism of chloride transport by band 3 using a ^{35}Cl NMR technique. We have previously shown that ^{35}Cl NMR can be used to: 1) observe chloride binding to band 3 transport sites on red cell membranes without interference from other chloride binding sites (2), and 2) resolve the transport sites into two populations on opposite sides of the membrane (4). The ^{35}Cl NMR assay for chloride binding sites is based on the fact that the ^{35}Cl NMR spectral width of chloride in a macromolecular binding site is typically at least 10^4 times larger than the line width of chloride in solution. Because of the large spectral width and relatively small concentration of bound chloride (in the present experiments [total protein]/[total chloride] $< 10^{-3}$), the observed ^{35}Cl NMR resonance is essentially that of solution chloride alone. However, when solution chloride samples macromolecular binding sites sufficiently rapidly, the sites can cause a measurable increase in the solution chloride line width. This increase in line width, or line broadening, can be shown by a theoretical analysis to be linearly related to the concentration of chloride binding sites (2, 13); moreover, we have experimentally verified this linear relationship in the red cell membrane-band 3 system (2). We have also shown that the line broadening due to band 3 transport sites can be isolated from the line broadening due to other chloride binding sites on red cell membranes using DNDS, an inhibitor of chloride binding to band 3 transport sites (2). Here the line broadening of the solution chloride ^{35}Cl NMR resonance is again used as an assay for chloride binding to band 3 transport sites.

The $^{35}Cl^-$ line broadening due to chloride binding sites contains a variety of information. Theoretical and experimental analysis indicates that the line broadening (δ) due to a heterogeneous population of chloride binding sites is given by Equation 1

$$\delta = \sum_j \alpha_j \frac{[E_jCl]}{[Cl^-]} \quad (1)$$

where the sum is over the different types of sites, α_j is a constant characteristic of the jth type of site, $[E_jCl]$ is the concentration of chloride bound to the jth type of site, and $[Cl^-]$ is the total or stoichiometric concentration of chloride in the sample. Equation 1 assumes that the bound chloride returns to solution before binding to another site, and that the concentration of bound chloride is negligible relative to the total chloride concentration. The line broadening due to the different sites is additive in Equation 1, and the contribution of the jth type of site to the line broadening is simply

$$\delta_j = \alpha_j \frac{[E_jCl]}{[Cl^-]} \quad (2)$$

which can be rewritten to yield

$$\delta_j = \frac{\alpha_j[E_j]_T}{K_{D_j}} \cdot \frac{[Cl^-]^{-1}}{[Cl^-]^{-1} + K_{D_j}^{-1}} \quad (3)$$

where $[E_j]_T$ is the total or stoichiometric concentration of binding sites and K_{D_j} is the microscopic dissociation constant for chloride binding (2). Equation 2 indicates that the line broadening is proportional to $[E_jCl]/[Cl^-]$, which is the fraction of total chloride that is bound to the jth type of site; Equation 3 indicates that the line broadening will yield a simple square hyperbola on a plot of line broadening *versus* $[Cl^-]^{-1}$. In both equations the quantity α_j contains information that depends on the physical situation (2): when the exchange of chloride between the binding site and solution is sufficiently fast, α_j depends on the characteristics of the jth type of site; in contrast, when the exchange is sufficiently slow, α_j depends only on the rate constant for dissociation of chloride from the jth type of site. Thus, for sites in the slow exchange limit, the line broadening can be used to study the dissociation of chloride from a chloride binding site. In short, the line broadening provides considerable insight into the molecular events that occur at the transport site.

Leaky Ghosts

Line Broadening Versus $[Cl^-]^{-1}$—The ability of the ^{35}Cl NMR technique to resolve band 3 transport sites on both sides of the membrane can be used to test models for the transport cycle. The membrane system used to observe simultaneously the inward- and outward-facing transport sites is the leaky ghost system, in which both orientations of the transport site make measurable contributions to the line broadening because the membranes have large holes that allow the bulk solution chloride to rapidly sample sites in both the internal and external compartments. We have previously shown that the transport site line broadening due to leaky ghosts is composed of approximately 60% outward-facing and 40% inward-facing line broadening (4).

The contributions made to the line broadening by the two

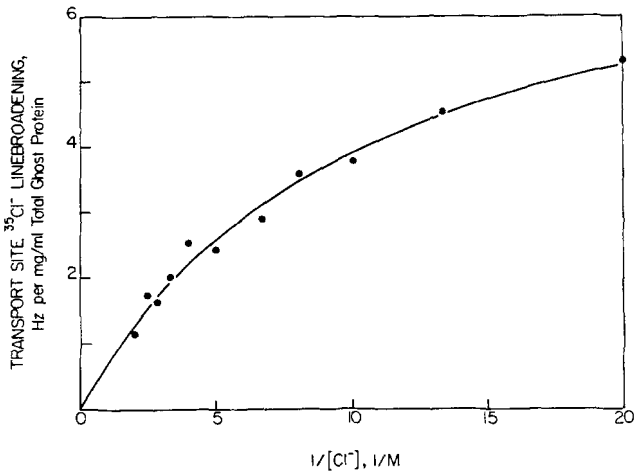

FIG. 1. **The $^{35}Cl^-$ line broadening due to inward- and outward-facing band 3 transport sites.** Shown is the DNDS-sensitive line broadening due to band 3 transport sites on leaky ghost membranes. The *solid curve* is the nonlinear least-squares curve calculated for a classical binding site or a ping-pong transporter with a best-fit macroscopic K_D of 90 ± 10 mM ($y = Ax/(x + K_D^{-1})$). Each sample contained the indicated [NH_4Cl] as well as 7.5 mM NaH_2PO_4, 20% D_2O, pH to 8.0 with NH_4OH. Sufficient citric acid (pH to 8.0 with NaOH) was added to bring the ionic strength up to that of the sample containing the highest [NH_4Cl] = 500 mM. Spectral parameters: 8.8 MHz, 3 °C and standard assay parameters (see text).

transport site orientations are additive (Equations 1–3). Thus, if the two orientations are completely independent, a plot of line broadening *versus* $[Cl^-]^{-1}$ for leaky ghost membranes will yield a sum of two square hyperbola, each for each orientation (Equation 3). However, the data obtained for leaky ghost membranes are well approximated by a single square hyperbola for which the best-fit macroscopic chloride dissociation constant is 90 ± 10 mM (Fig. 1). At first glance this macroscopic homogeneity appears to contradict a variety of evidence suggesting that the characteristics of the inward- and outward-facing transport sites are different (see Introduction).

The ping-pong model can explain the observation of a single square hyperbola. For a ping-pong transporter, the steady-state transmembrane fluxes of occupied transport sites are equal for the two opposing directions (Appendix I).

$$k_{IO}[E_ICl] = k_{OI}[E_OCl] \tag{4}$$

Here we have used $[E_xCl]$ to denote the concentration of occupied transport sites on side x, and k_{xy} to denote the rate constant for translocation from side x to side y. Thus, the distribution of occupied transport sites $[E_OCl]/[E_ICl]$ is governed by the ratio of the translocation rate constants (k_{IO}/k_{OI}). This constraint on the occupied site distribution leads to a well-defined averaging of the microscopic constants of the inward- and outward-facing sites so that the line broadening due to transport sites on both sides of the membrane is given by (Appendix I[2]):

$$\delta = \frac{\tilde{\alpha}[E]_T}{\overline{K_D}} \cdot \frac{[Cl]^{-1}}{[Cl^-]^{-1} + \overline{K_D}^{-1}} \tag{5}$$

where $[E]_T$ is the total concentration of band 3 transport units, and $\tilde{\alpha}$ and $\overline{K_D}$ are macroscopically observed constants defined by

$$\tilde{\alpha} = \alpha_I\omega_I + \alpha_O\omega_O$$

and

$$\overline{K_D} = K_{D_I}\omega_I + K_{D_O}\omega_O \tag{6}$$

These macroscopic constants are weighted averages of the corresponding microscopic constants for the inward (subscript I)- or outward (subscript O)-facing transport sites. The weighting factors in these averages are

$$\omega_I = \frac{\tau_{IO}}{\tau_{IO} + \tau_{OI}}, \qquad \omega_O = \frac{\tau_{OI}}{\tau_{IO} + \tau_{OI}} \tag{7}$$

where the quantities τ_{xy} are the inverse rate constants for the x to y translocation ($\tau_{xy} = 1/k_{xy}$). The form of the weighting factors confirms the idea that the averaging is due to the special transport site distribution defined by Equation 4; assuming that the vast majority of transport sites are facing either side x or side y rather than actively undergoing translocation at any given point in time, ω_x is simply the fraction of occupied sites found on side x (Equation 4).

Thus, the ping-pong mechanism couples the inward- and outward-facing transport site populations in such a way that the macroscopic characteristics of these sites appear to stem from a homogeneous population. This idea can be tested further by examining the macroscopic behavior of transport sites in the presence of varying bromide concentration or pH.

Line Broadening Versus [Br^-]—Bromide can be transported across the membrane in both directions by band 3 (8); thus, it must bind to both orientations of the transport site. Bromide binding is also known to competitively inhibit chloride binding to the transport site (6). Consistent with this picture is the observation that bromide completely inhibits the line broadening due to band 3 transport sites on both sides of leaky ghost membranes (Fig. 2). However, despite the fact that the characteristics of the inward- and outward-facing transport sites appear to be different (see Introduction), a

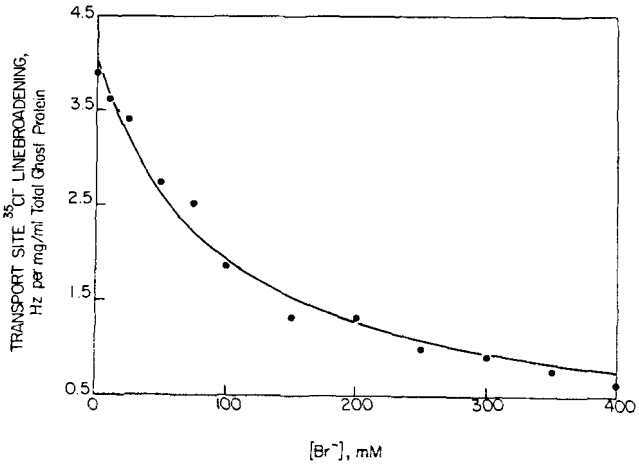

FIG. 2. **The effect of Br^- on the $^{35}Cl^-$ line broadening due to inward- and outward-facing band 3 transport sites.** Shown is a titration with Br^- of the DNDS-sensitive line broadening due to band 3 transport sites. The *solid line* is a nonlinear least-squares curve calculated for a classical binding site or a ping-pong transporter with a best-fit macroscopic K_D of 90 ± 10 mM ($y = A(1 - x/(x + K_D))$). Each sample contained the indicated concentration of NaBr, as well as 100 mM NaCl, 2.5 mM NaH_2PO_4, 20% D_2O, pH to 8.0 with NaOH. Spectral parameters: 8.8 MHz, 3 °C and standard assay parameters (see text).

[2] Portions of this paper (including Appendices I and II) are presented in miniprint at the end of this paper. Miniprint is easily read with the aid of a standard magnifying glass. Full size photocopies are available from the Journal of Biological Chemistry, 9650 Rockville Pike, Bethesda, MD 20814. Request Document No. 85M-0940, cite the authors, and include a check or money order for $3.60 per set of photocopies. Full size photocopies are also included in the microfilm edition of the Journal that is available from Waverly Press.

plot of line broadening *versus* [Br^-] (Fig. 2) for leaky ghost membranes is well approximated by a curve drawn for a homogeneous population of sites, where the macroscopic inhibitor constant for bromide is 90 ± 10 mM in the presence of 100 mM chloride. Completely analogous results have been obtained for fluoride, iodide, and bicarbonate, which are also competitive inhibitors that bind to both orientations of the transport site (2, 6).

The macroscopic transport site homogeneity observed in experiments with competitive inhibitors is predicted by the ping-pong model. For a ping-pong transporter, the transport site line broadening due to the inward- and outward-facing transport sites is (Appendix I):

$$\delta = \delta(O)\left(1 - \frac{[X]}{[X] + \overline{K_X}}\right) \tag{8}$$

where $\delta(O)$ is the transport site line broadening in the absence of inhibitor, $[X]$ is the inhibitor concentration, and $\overline{K_X}$ is defined by

$$\overline{K_X} = \frac{K_{D_I}\omega_I + K_{D_O}\omega_O + [Cl^{-1}]}{(K_{D_I}/K_{X_I})\omega_I + (K_{D_O}/K_{X_O})\omega_O} \tag{9}$$

The macroscopic quantity K_X is a weighted average of the microscopic constants K_{X_I} and K_{X_O} for inhibitor binding to the inward- and outward-facing site, respectively. This average is more complicated than that for simple chloride binding (Equations 5 and 6) because for an inhibitor that competes with chloride for binding, the macroscopic inhibitor constant is a function of the chloride concentration. However, it is clear that macroscopic homogeneity remains a characteristic feature of the behavior of transport sites in the presence of competitive inhibitors.

For completeness we have also derived an expression for the $\overline{K_X}$ of a competitive inhibitor that only binds to one orientation of the transport site, as does DNDS (Appendix I).

Line Broadening versus pH—Band 3-catalyzed chloride transport is inhibited at pH > 11 in a reversible fashion (14), suggesting that the transport site contains at least one essential positive charge necessary for substrate binding. In the present experiments the pH dependence of the transport site line broadening is studied using sonicated leaky ghost membranes which, like the leaky ghost system, enable observation of the line broadening of both inward- and outward-facing transport sites (4). Leaky ghosts are not used because at pH > 10 such membranes spontaneously break up to form vesicles (15) which, if sealed, would hide the intravesicular transport sites (4). The transport site line broadening due to sonicated ghosts is inhibited by high pH (Fig. 3); this inhibition is not due to simple denaturation of the protein since the inhibition is removed by back-titration with acid (Table I). The base titration is well approximated by a titration curve drawn for a homogeneous population of sites that have a macroscopic $\overline{pK_A}$ = 11.1 ± 0.1 in the presence of 250 mM chloride (Fig. 3).

The behavior of the transport site in this base titration is another example of the macroscopic homogeneity predicted by the ping-pong model. For a ping-pong transporter the base titration of the transport site line broadening is described by (Appendix I):

$$\delta = \delta(O)\left(1 - \frac{10^{pH}}{10^{pH} + 10^{\overline{pK_A}}}\right) \tag{10}$$

where $\delta(O)$ is the line broadening when the essential positive charge is intact (pH ≪ $\overline{pK_A}$), and the macroscopically observed $\overline{pK_A}$ is

$$\overline{pK_A} = \log_{10}\frac{K_{D_I}\omega_I + K_{D_O}\omega_O + [Cl^-]}{K_{A_I}K_{D_I}\omega_I + K_{A_O}K_{D_O}\omega_O} \tag{11}$$

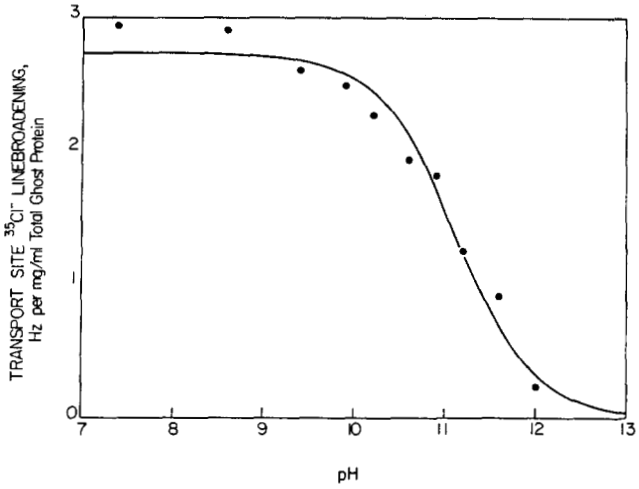

FIG. 3. **The effect of pH on the $^{35}Cl^-$ line broadening due to inward- and outward-facing band 3 transport sites.** Shown is a base titration of the DNDS-sensitive line broadening due to band 3 transport sites. The *solid line* is a nonlinear least-squares curve generated for a classical binding site or a ping-pong transporter with a best-fit macroscopic pK_A of 11.1 ± 0.1. The samples contained 250 mM NaCl, 2.5 mM NaH_2PO_4, 20% D_2O, pH adjusted to the indicated value with NaOH or HCl. Spectral parameters: 8.8 MHz, 3 °C and standard assay parameters.

TABLE I

Reversibility of the high pH inhibition of transport site line broadening in the sonicated ghost system

Treatment	$^{35}Cl^-$ line broadening due to sonicated ghosts		$^{35}Cl^-$ line broadening due to band 3 transport sites
	A (no DNDS)	B (1 mM DNDS)	A-B
	Hz/mg/ml total membrane protein		
None (pH 8.0)	7.1 ± 0.3	4.2 ± 0.1	2.9
pH 12.2, then pH 8.0	7.3 ± 0.3	5.6 ± 0.3	2.7

Thus, the macroscopic titration of a transport site positive charge necessary for chloride binding is described by the quantity $\overline{pK_A}$, which is a weighted average of the microscopic quantities pK_{A_I} and pK_{A_O} for the inward- and outward-facing transport sites, respectively. The average is more complicated than that for simple chloride binding (Equations 5 and 6) because it is assumed that chloride binding protects the transport site from deprotonation; as a result the $\overline{pK_A}$ depends on the chloride concentration (Appendices I and II).

The measured $\overline{pK_A}$ also provides some insight into the identity of the essential positive charge in the transport site. The observed value of $\overline{pK_A}$ = 11.1 ± 0.1 is sufficiently large to suggest that one or both of the transport site conformations contains an essential arginine residue and no essential lysine residues. However, this value is significantly less than the value of 12.0 obtained for the outward-facing transport site in kinetic experiments at the same chloride concentration (250 mM chloride (14)). Since the macroscopic quantity $\overline{pK_A}$ is an average of the microscopic pK_A values of the two orientations of the transport site (Equation 11), it follows that the inward-facing site must satisfy $pK_{A_I} < \overline{pK_A} = 11.1 \pm 0.1$. These results are completely consistent with the previous conclusion that the positive charge in the outward-facing transport site is provided by arginine (1, 9), but no conclusion

can be made concerning the identity of the inward-facing positive charge, which could be an arginine or lysine.

Crushed Ghosts: Dissociation of Chloride from the Outward-facing Transport Site

For a classical binding site, the rate constant for dissociation of substrate from the site is independent of the substrate concentration. This rate constant can be studied for chloride dissociation from the outward-facing transport site of band 3 because this site is in the slow exchange limit where the line broadening is a function of the rate constant for chloride dissociation (see Ref. 10). Here the dependence of the macroscopically observed rate constant for chloride dissociation from the outward-facing transport site will be examined as a test of models for the transport cycle.

In order to specifically monitor the line broadening due to the outward-facing transport site, crushed ghost membranes have proven particularly useful. These membranes, which are prepared from leaky ghost membranes, are permanently collapsed by large centripetal forces experienced during centrifugation. After crushing, the membranes give rise to a transport site line broadening composed solely of the contribution from the outward-facing sites. The line broadening due to inward-facing transport sites is not observed because the intracellular compartment makes a negligible contribution to the ^{35}Cl NMR resonance, both due to the slowness of exchange between the intracellular and extracellular compartments and to the relatively small size of the intracellular compartment (4).

The line broadening due to the outward-facing transport site has been shown to be in the slow exchange limit using crushed ghosts and also right-side-out vesicles (see Ref. 10); as a result the factor α_j in the line broadening (Equations 2 and 3) is given by Equation 12

$$\alpha_j = \overline{k_{OFF}}/\pi \tag{12}$$

Here $\overline{k_{OFF}}$ is an average over all of the outward-facing transport sites of the microscopic chloride dissociation constant k_{OFF}, which is defined for a single outward-facing transport site (E_O) by the reaction

$$E_O + Cl^- \underset{k_{OFF}}{\overset{k_{ON}}{\rightleftharpoons}} E_OCl \tag{13}$$

Thus, $\overline{k_{OFF}}$ is a macroscopic rather than a microscopic quantity whenever heterogeneity exists in k_{OFF}. For a classical chloride binding site $\overline{k_{OFF}} = k_{OFF}$ is a constant that is independent of the chloride concentration. In such a case α_j is also a constant (Equation 12), and a square hyperbola is observed on a plot of line broadening *versus* $[Cl^-]^{-1}$ (Equation 3). For crushed ghost membranes, a plot of transport site line broadening *versus* $[Cl^-]^{-1}$ is well approximated by a square hyperbola, indicating that the outward-facing transport site behaves like a classical chloride binding site.

This classical behavior is predicted by the ping-pong model, for which the line broadening due to outward-facing transport sites is given by (Appendix I):

$$\delta_O = \frac{k_{OFF}[E]_T}{\pi \overline{K_D}} \cdot \frac{\tau_{OI}}{\tau_{OI} + \tau_{IO}} \cdot \frac{[Cl^-]^{-1}}{[Cl^-]^{-1} + \overline{K_D}^{-1}} \tag{14}$$

where k_{OFF} is the microscopic off-rate constant for the outward-facing transport site, $[E]_T$ is the total concentration of band 3 transport units, $\overline{K_D}$ is the macroscopic chloride dissociation constant (Equation 6), and τ_{xy} is the inverse of the rate constant for the translocation of the chloride-transport site complex from side x to side y (Equation 7). Thus, while

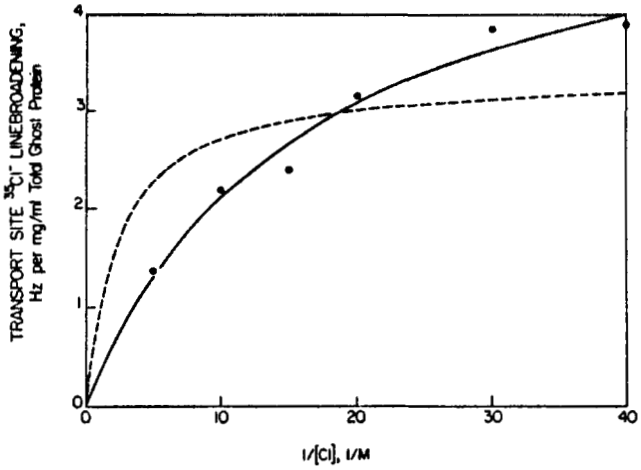

FIG. 4. **The $^{35}Cl^-$ line broadening due to outward-facing band 3 transport sites.** The DNDS-sensitive line broadening due to band 3 transport sites was determined using crushed ghost membranes. The *solid curve* is the nonlinear least-squares best-fit curve for a classical binding site or a ping-pong transporter with a macroscopic K_D of 60 ± 10 mM ($y = Ax/(x + K_D^{-1})$). The *dashed curve* is the nonlinear least-squares best-fit curve for a special case of the two-site ordered sequential model (16), assuming that the transport site $K_D = 80$ mM (17) and the second site $K_{D'} = 340$ mM. Experimental details exactly as described in Fig. 1 legend, except that the ionic strength was brought to 200 mM, the highest $[NH_4Cl]$ used here.

the classical behavior of the outward-facing transport site on crushed ghosts strongly disfavors any model in which $\overline{k_{OFF}}$ is a function of the chloride concentration within the range 25 mM ≤ $[Cl^-]$ ≤ 200 mM (16), such classical behavior is completely consistent with the ping-pong model.

The ping-pong model is also consistent with the discrepancy between the values measured for the apparent chloride dissociation constant of the outward-facing transport site in 1) the crushed ghost system ($\overline{K_{D_O}} = 60 \pm 10$ mM, Fig. 4), and 2) the chloride-loaded intact red cell system ($\overline{K_{D_O}} = 4$ mM (8)). In the crushed ghost system the chloride concentration is identical in the internal and external compartments so that $\overline{K_{D_O}}$ for a ping-pong transporter contains contributions from the microscopic dissociation constants of both the inward- and outward-facing sites ($\overline{K_{D_O}} = K_{D_O}\omega_O + K_{D_I}\omega_I$, Equations 5 and 6 for $\alpha_I = 0$. In contrast, in the chloride-loaded system where intact red cells are loaded with sufficient chloride to nearly saturate the inward-facing transport site, the $\overline{K_{D_O}}$ of a ping-pong transporter depends upon the microscopic dissociation constant of the outward-facing site alone ($\overline{K_{D_O}} = K_{D_O}\omega_O$, Equations 6 and A7). As previously noted for a ping-pong transport mechanism, the observation that $\overline{K_{D_O}}$ in the chloride-loaded systems ($K_{D_O}\omega_O$) is significantly smaller than in equilibrium systems ($K_{D_O}\omega_O + K_{D_I}\omega_I$) indicates that there is an inherent asymmetry in the affinity of the inward- and outward-facing transport sites for chloride ($K_{D_O} < K_{D_I}$ (8)); and/or there is an inherent asymmetry in the time that an occupied transport site waits before translocating to the opposite conformation ($\tau_{OI} < \tau_{IO}$ (9)). Thus, the present results re-emphasize the importance of asymmetry in the band 3 ping-pong transport cycle, although this asymmetry is generally hidden by averaging of the microscopic characteristics of the inward- and outward-facing transport sites (Equations 6, 9, and 11).

DISCUSSION

In general, previously published mechanistic studies of band 3 using kinetic techniques have yielded results that are com-

pletely consistent with a ping-pong mechanism (reviewed in Refs. 1, 9, and 18); for an exception see (16)). Despite this pre-existing strong body of evidence in favor of the ping-pong model, it still appears useful to test the mechanism using independent approaches; thus, we have employed ^{35}Cl NMR to examine the transport mechanism. The ^{35}Cl NMR technique circumvents several difficulties of technique or interpretation that have been encountered previously: 1) chloride is a rapidly transported physiological anion that must be transported via the physiological band 3 mechanism; thus the possible significance of competing mechanisms that could become important for slowly transported, nonphysiological substrates is minimized, 2) the membrane systems utilized here are leaky; thus potential complications due to transmembrane ionic, electrical, and pH gradients are nonexistent, and 3) the modifier effect is not observed in studies of chloride binding to band 3; thus complications due to this effect are avoided.

The ability of the ^{35}Cl NMR technique to resolve band 3 transport sites on opposite sides of the membrane has made possible several tests of the mechanism of chloride transport, and in each case the ping-pong model is completely consistent with the data. For instance, the ping-pong model predicts that a population of transport sites will be distributed among the inward- and outward-facing conformations unless they are all recruited to one conformation by appropriate experimental conditions. The ^{35}Cl NMR technique has confirmed the existence of both transport site conformations in the unperturbed system; also, the technique has allowed observation of transport site recruitment to the outward-facing conformation by DNDS (4). The present application of ^{35}Cl NMR focuses on the characteristics of the mixed population of inward- and outward-facing transport sites. The ping-pong model predicts that the microscopic characteristics of the inward- and outward-facing conformations will be averaged due to the special way that a steady state population of transport sites is distributed between the inward- and outward-facing states; as a result the inward- and outward-facing transport sites will together appear to be a homogeneous population in macroscopic experiments. Such macroscopic homogeneity is indeed observed; the transport sites exhibit a single affinity for chloride or bromide, studied here, as well as for fluoride, iodide, and bicarbonate (2). Similarly, the transport sites exhibit a single pK_A for titration with base. Thus, the ping-pong model is both qualitatively and quantitatively consistent with all of the available ^{35}Cl NMR evidence.

The conclusion that band 3 is a ping-pong transporter allows the chemical equation of the anion transport cycle to be specified. For a ping-pong transporter, the simplest possible chemical equation for chloride self-exchange is:

$$E_I + Cl_I^- \underset{k_2}{\overset{k_1}{\rightleftharpoons}} E_ICl \underset{k_4}{\overset{k_3}{\rightleftharpoons}} E_OCl \underset{k_6}{\overset{k_5}{\rightleftharpoons}} E_O + Cl_O^- \qquad (15)$$

where E represents the band 3 transport site, and the subscripts I and O represent the inside and outside compartments. As already discussed, this chemical equation is consistent with a range of kinetic and ^{35}Cl NMR results. This chemical equation also contains the fundamental features of the ping-pong transport cycle; the transport unit has a single transport site that is alternately exposed to opposite sides of the membrane, and the site can only reorient when it contains bound anion. These and other fundamental features of the band 3 transport cycle are further discussed in the following paper, which focuses on the rate constants k_1–k_6 in the transport cycle.

REFERENCES

1. Macara, I. G., and Cantley, L. C. (1983) *Cell Membr. Methods Rev.* **1,** 41–87
2. Falke, J. J., Pace, R. J., and Chan, S. I. (1984) *J. Biol. Chem.* **259,** 6472–6480
3. Jennings, M. L. (1982) *J. Gen. Physiol.* **79,** 169–185
4. Falke, J. J., Pace, R. J., and Chan, S. I. (1984) *J. Biol. Chem.* **259,** 6481–6491
5. Cass, A., and Dalmark, M. (1973) *Nat. New Biol.* **244,** 47–49
6. Dalmark, M. (1976) *J. Gen. Physiol.* **67,** 223–234
7. Knauf, P. A., Law, F.-Y., Tarshis, T., and Furuya, W. (1984) *J. Gen. Physiol.* 83, 683–701
8. Gunn, R. B., and Frölich, O. (1979) *J. Gen. Physiol.* **74,** 351–374
9. Knauf, P. A. (1979) *Curr. Top. Membr. Transp.* **12,** 249–363
10. Falke, J. J., Kanes, K. J., and Chan, S. I. (1985) *J. Biol. Chem.* **260,** 9545–9551
11. Lowry, O. H., Rosebrough, N. J., Farr, A. L., and Randall, R. J. (1951) *J. Biol. Chem.* **193,** 265–275
12. Markwell, M. A., Haas, S. M., Bieber, L. L., and Tolbert, N. E. (1978) *Anal. Bioch.* **87,** 206–210
13. Forsén, S., and Lindman, B. (1981) *Methods Biochem. Anal.* **27,** 289–486
14. Wieth, J. O., and Bjerrum, P. J. (1982) *J. Gen. Physiol.* **79,** 253–282
15. Steck, T. L. (1974) *Methods Membr. Biol.* **2,** 245–281
16. Salhany, J. M., and Rauenbeuhler, P. B. (1983) *J. Biol. Chem.* **258,** 245–249
17. Brazy, P. C., and Gunn, R. B. (1976) *J. Gen. Physiol.* **68,** 583–599
18. Gunn, R. B., and Frölich, O. (1982) *Chloride Transport in Biological Membranes* (Zadunaisky, J. A., ed) Academic Press, New York
19. Frölich, O., and Gunn, R. B. (1981) *Adv. Physiol. Sci.* **6,** 275–280
20. Fröhlich, O. (1982) *J. Membr. Biol.* **65,** 111–123

Supplementary Material to

EVIDENCE THAT ANION TRANSPORT BY BAND 3 PROCEEDS VIA A PING-PONG MECHANISM INVOLVING A SINGLE TRANSPORT SITE. A ^{35}Cl NMR STUDY.

Joseph J. Falke and Sunney I. Chan

APPENDIX I. THE PING-PONG MODEL

INTRODUCTION

The following discussion presents a mathematical treatment of the ping-pong model. In particular, the linebroadening due to the transport sites of a ping-pong transporter is examined as a function of varying: 1) chloride concentration, 2) inhibitor concentration, and 3) pH.

Definitions. The subscripts O and I are used to represent the outside (extracellular) and inside (intracellular) compartments, and symbols for ionic charges and concentration brackets are understood rather than expressly written. For instance, Cl_O and H_O denote the chloride and hydrogen concentrations in the outside compartment, respectively.

Conditions. Only leaky membranes are utilized here; thus, the following conditions hold: $Cl_I = Cl_O = Cl$ and $H_I = H_O = H$. Also the concentration of chloride binding sites is negligible relative to the total (stoichiometric) chloride concentration, so the free and total chloride concentrations are essentially identical.

Fundamental Characteristics of a Ping-Pong Transporter. This model proposes that the transport unit has a single transport site that binds a chloride ion on one side of the membrane; only then is the site able to cross the membrane. We make the reasonable assumption that the distribution of outward- and inward-facing transport sites reaches a kinetic steady state before this experiment begins. (The chloride translocation time is $\leq$ 2 msec per turnover at 0° C (19).) Under these conditions, the flux of binding sites from outside to inside must cancel the opposing flux, or

$$k_{OI}(E_OCl) + k'_{OI}(E_O) = k_{IO}(E_ICl) + k'_{IO}(E_I) \tag{A1}$$

Here k_{xy} is the rate constant for the side x to side y translocation. E_x is the concentration of empty transport sites on side x, and E_xCl is the concentration of occupied transport sites on side x. For a perfect ping-pong transporter the rate constants for empty site translocation are $k_{OI} = k_{IO} = 0$. In this limit the transport site interconversion is described by the equilibrium $E_OCl \rightleftharpoons E_ICl$ and Equation A1 becomes

$$k_{OI}E_OCl = k_{IO}E_ICl \tag{A2}$$

For a ping-pong transporter, then, the distribution of bound chloride between the two sides of the membrane is determined solely by the rates of chloride translocation. This characteristic behavior of the ping-pong model has been previously described (8,9).

THE $^{35}Cl^-$ LINEBROADENING DUE TO A PING-PONG TRANSPORTER: DEPENDENCE ON $[Cl^-]^{-1}$

The microscopic dissociation constant for chloride binding to transport sites will be different on the two sides of the membrane if the inward- and outward-facing transport sites have different structures. However, the following discussion shows that a ping-pong transporter will always exhibit a single macroscopic dissociation constant (K_D) for chloride binding in linebroadening experiments, even though the microscopic chloride dissociation constant may be different for the inward- and outward-facing sites.

Useful Relationships and Assumptions. Use will be made of the familiar expressions for K_{D_O}, the microscopic dissociation constant for chloride binding to the outward-facing transport site, and P_O, the fraction of these sites that contains bound chloride:

$$K_{D_O} = \frac{(E_O)(Cl_O)}{E_OCl} \tag{A3}$$

$$P_O = \frac{E_OCl}{N_O} = \frac{Cl_O}{Cl_O + K_{D_O}} \tag{A4}$$

where N_O is the total or stoichiometric concentration of outward-facing transport sites. Analogous expressions can be written for inward-facing transport sites. The validity of Equations A3 and A4 assumes that dissociation is the only significant pathway available to a bound chloride ion; thus, the dissociation rate must be sufficiently rapid compared to the translocation rate. This assumption is justified in the following paper.

The Concentration of Occupied Transport Sites. In order to determine the linebroadening due to transport sites (or, in kinetic studies, the rate of transport), the concentration of the transport sites must be determined. This quantity can be derived by first substituting Equation A4 into Equation A1 to yield

$$k_{OI}N_OP_O = k_{IO}N_IP_I \tag{A5}$$

Rearrangement of this expression yields the concentration of outward-facing transport sites:

$$N_O = \left(\frac{k_{IO}}{k_{OI}}\right)\left(\frac{P_I}{P_O}\right)N \Big/ \left(1 + \frac{k_{IO}}{k_{OI}}\frac{P_I}{P_O}\right) \tag{A6}$$

where $N = N_O + N_I$ is the total concentration of occupied and unoccupied transport sites, irrespective of sidedness. Substitution of Equation A4 for N_O yields

$$E_OCl = \left(\frac{k_{IO}}{k_{OI}}\right)(P_I)\,N \Big/ \left(1 + \frac{k_{IO}}{k_{OI}}\frac{P_I}{P_O}\right) \tag{A7}$$

Finally, substitution of Equation A4 for P_O and P_I under the condition $Cl_O = Cl_I = Cl$ yields the concentration of occupied outward-facing transport sites:

$$E_OCl = \left(\frac{k_{IO}}{k_{OI}}\right)\left(\frac{Cl}{Cl + K_{D_I}}\right)N \Big/ \left(1 + \frac{k_{IO}}{k_{OI}}\frac{Cl + K_{D_O}}{Cl + K_{D_I}}\right) \tag{A8}$$

An expression for E_ICl can be derived in an analogous way.

The Transport Site Linebroadening. The total $^{35}Cl^-$ linebroadening due to a heterogeneous population of independent binding sites is given by

$$\delta = \sum_j \alpha_j \left(\frac{E_jCl}{Cl}\right) \tag{A9}$$

where E_jCl is the stoichiometric concentration of chloride bound to the j^{th} type of site, and α_j is a constant characteristic of the j^{th} type of site. The α_j of the transport site could be different in its inward- and outward-facing conformations; thus, the transport site linebroadening is

$$\delta = \alpha_O\left(\frac{E_OCl}{Cl}\right) + \alpha_I\left(\frac{E_ICl}{Cl}\right) \tag{A10}$$

Substitution of Equation A8 for E_OCl and an analogous expression for E_ICl followed by rearrangement yields the following simple expression for the transport site linebroadening:

$$\delta = \frac{N\bar{\alpha}}{Cl + \bar{K}_D} \tag{A11}$$

where the macroscopically observed quantities $\bar{\alpha}$ and $\bar{K}_D$ are

$$\bar{\alpha} = \left(\frac{\alpha_O}{k_{OI}} + \frac{\alpha_I}{k_{IO}}\right) \Big/ \left(\frac{1}{k_{OI}} + \frac{1}{k_{IO}}\right) \tag{A12}$$

$$\bar{K}_D = \left(\frac{K_{D_O}}{k_{OI}} + \frac{K_{D_I}}{k_{IO}}\right) \Big/ \left(\frac{1}{k_{OI}} + \frac{1}{k_{IO}}\right) \tag{A13}$$

Multiplication and division of Equation A11 with $(Cl\bar{K}_D)^{-1}$ finally yields

$$\delta = \frac{N\bar{\alpha}}{\bar{K}_D} \cdot \frac{Cl^{-1}}{Cl^{-1} + \bar{K}_D^{-1}} \tag{A14}$$

Thus, the ping-pong model predicts that the transport sites will behave like a homogenous class of sites in linebroadening experiments with the macroscopically observed quantities $\bar{\alpha}$ and $\bar{K}_D$ given by the weighted average of the microscopic constants for the inward- and outward-facing transport sites.

THE $^{35}Cl^-$ LINEBROADENING DUE TO A PING-PONG TRANSPORTER: EFFECTS OF REVERSIBLE INHIBITORS

The linebroadening due to the transport sites of a ping-pong transporter is a function of the concentration of inhibitors, here the form of this function is derived for different types of reversible inhibitors. Special attention is given to the reversible transport site inhibitors that have been examined in this paper or elsewhere (2): Br^-, I^-, HCO_3^-, F^-, and p-nitrobenzene sulfonate. The expressions that are derived are general results of the ping-pong model and are applicable to linebroadening or kinetic experiments in a variety of red cell membrane experiments.

Useful Relationships and Assumptions. Consider an inhibitor of the linebroadening due to transport sites: the most general case is that of the mixed inhibitor that can bind either to an empty (E) or occupied (ECl) transporter. Thus, for each side of the membrane, two inhibitor constants are required to explain inhibitor (X) binding:

$$K_{X_O} = \frac{(E_O)(X)}{E_OX} \tag{A15}$$

$$K'_{X_O} = \frac{(E_OCl)(X)}{E_OClX} \tag{A16}$$

Analogous expressions can be written for the inside compartment. Here it will be assumed that when an inhibitor binds to a particular transporter, it completely eliminates the transport site linebroadening from that transporter but has no effect on other transporters. In this case the transport site linebroadening is given by

$$\delta = \delta(0)\,(1 - P_x) \tag{A17}$$

where $\delta(0)$ is the transport site linebroadening in the absence of inhibitor, and P_x is the fraction of the band 3 population which is inhibited.

Dependence of the Fractional Inhibition on the Inhibitor Concentration. The fractional inhibition is simply the concentration of the band 3-inhibitor complex divided by the total band 3 concentration:

$$P_x = \frac{E_OX + E_IX + E_OClX + E_IClX}{E_O + E_I + E_OCl + E_ICl + E_OX + E_IX + E_OClX + E_IClX} \tag{A18}$$

Using 1) the definitions of K_{D_O} (Equation A3), K_{X_O} (Equation A15), K'_{X_O} (Equation A16), 2) the corresponding definitions for the inside compartment, and 3) Equation A2, the fractional inhibition can be written as

$$P_x = \frac{\left\{\frac{X_O}{K'_{X_O}} + \frac{X_I}{K'_{X_I}}\cdot\frac{k_{OI}}{k_{IO}} + \frac{X_O}{K_{X_O}}\cdot\frac{K_{D_O}}{Cl_O} + \frac{X_I}{K_{X_I}}\cdot\frac{K_{D_I}}{Cl_I}\cdot\frac{k_{OI}}{k_{IO}}\right\}}{1 + \frac{k_{OI}}{k_{IO}} + \frac{K_{D_O}}{Cl_O} + \frac{K_{D_I}}{Cl_I}\cdot\frac{k_{OI}}{k_{IO}} + \left\{\quad\right\}} \tag{A19}$$

When $X_O = X_I = X$, this expression reduces to the simple form

$$P_x = \frac{X}{X + \bar{K}_X} \tag{A20}$$

where the macroscopically observed inhibitor constant is

$$\bar{K}_X = \frac{1 + \frac{k_{OI}}{k_{IO}} + \frac{K_{D_O}}{Cl_O} + \frac{K_{D_I}}{Cl_I}\cdot\frac{k_{OI}}{k_{IO}}}{\frac{1}{K'_{X_O}} + \frac{1}{K'_{X_I}}\cdot\frac{k_{OI}}{k_{IO}} + \frac{1}{K_{X_O}}\cdot\frac{K_{D_O}}{Cl_O} + \frac{1}{K_{X_I}}\cdot\frac{K_{D_I}}{Cl_I}\cdot\frac{k_{OI}}{k_{IO}}} \tag{A21}$$

and when $Cl_O = Cl_I = Cl$, rearrangement yields

$$\bar{K}_X = \frac{\frac{K_{D_O}}{k_{OI}} + \frac{K_{D_I}}{k_{IO}} + Cl\left(\frac{1}{k_{OI}} + \frac{1}{k_{IO}}\right)}{\frac{K_{D_O}}{K_{X_O}k_{OI}} + \frac{K_{D_I}}{K_{X_I}k_{IO}} + Cl\left(\frac{1}{K_{X_O}k_{OI}} + \frac{1}{K_{X_I}k_{IO}}\right)} \tag{A22}$$

This expressions indicates that $\bar{K}_X$ depends on all of the inhibitor's microscopic dissociation constants. Also present are the quantities Cl, K_{D_O}, K_{D_I} and k_{xy} because 1) chloride binding can change the overall affinity of the transporter for the inhibitor, and 2) varying chloride concentration can change the distribution of transport sites across the membrane unless $K_{D_O} = K_{D_I}$ (Equation A6).

Competing Substrates. Inhibitors of this class act by binding to the transport site, thereby preventing chloride binding. Such inhibitors cannot bind to the site when it is occupied by chloride so the microscopic dissociation constants K'_{X_I} and K'_{X_O} can be neglected ($1/K'_{X_O} = 1/K'_{X_I} = 0$, Equation A16). In this case $\bar{K}_X$ becomes

$$\bar{K}_X = \left(\frac{K_{D_O}}{k_{OI}} + \frac{K_{D_I}}{k_{IO}} + Cl\left(\frac{1}{k_{OI}} + \frac{1}{k_{IO}}\right)\right) \Big/ \left(\frac{K_{D_O}}{K_{X_O}k_{OI}} + \frac{K_{D_I}}{K_{X_I}k_{IO}}\right) \tag{A23}$$

This expression describes the macroscopically observed $\bar{K}_X$ for competing substrates that bind to both the inward- and outward- facing transport sites. The inhibitors of this type that we have studied by $^{35}Cl^-$ NMR are Br^- (see text), I^-, F^- and HCO_3^- (2).

Side-Specific Inhibitors. A competitive inhibitor of chloride binding to the transport site that only binds to the outward-facing orientation ($1/K_{X_I} = 0$) further simplifies Equation A23:

$$\bar{K}_X = K_{X_O}\left[1 + \frac{K_{D_I}}{K_{D_O}}\cdot\frac{k_{OI}}{k_{IO}} + \frac{Cl}{K_{D_O}}\left(1 + \frac{k_{OI}}{k_{IO}}\right)\right] \tag{A24}$$

This equation as well as Equation A23 predicts that the chloride dependence of $\bar{K}_X$ will have the form

$$\bar{K}_X = C_1 + C_2Cl \tag{A25}$$

as has been experimentally observed for DNDS by Frölich (20) and verified by our laboratory (to be published). This experimental result suggests that the binding of chloride and DNDS are mutually exclusive since an inhibitor that can bind to a transporter containing chloride will give rise to a more complicated expression ($1/K_X > 0$, Equation A22).

THE $^{35}Cl^-$ LINEBROADENING DUE TO A PING-PONG TRANSPORTER: EFFECTS OF pH

If the transport site contains a titratable positive charge that is required for chloride binding, then the linebroadening due to the site will be inhibited when the charge is removed by sufficiently high pH. As shown below, a ping-pong transporter will titrate at high pH with a single macroscopically observed pK_A, even if the microscopic pK_A for the transport site is different on the two sides of the membrane. The expressions that are derived are general results of the ping-pong model and are applicable to linebroadening or kinetic experiments with any type of red cell membrane preparation.

Useful Relationships and Assumptions. Consider a ping-pong transporter with the following characteristics. 1) the transport site contains a titratable positive charge to which substrate anion binds, and 2) neutralization of the transport site eliminates chloride binding.

In order to clarify the presentation, the transport site concentration on side x will be written E_xH for intact sites and E_x for base neutralized sites. Thus, the concentration of chloride bound to transport sites is now written E_xHCl instead of the previous terminology E_xCl. The chloride dissociation constant for the outward-facing transport site can therefore be written

$$K_{D_O} = \frac{(E_OH)(Cl_O)}{E_OHCl} \tag{A26}$$

where it is assumed, as for Equation A4, that dissociation is the only significant pathway available to the bound chloride ion. Thus, the dissociation rate must be very rapid compared to the transport rate; this assumption is justified in the following paper (10). The proton dissociation constant can be written

$$K_{A_O} = \frac{(E_O)(H)}{(E_OH)} \tag{A27}$$

Analogous expressions can be written for the inward-facing transport sites; also in this terminology Equation A2 becomes

$$k_{OI}(E_OHCl) = k_{IO}(E_IHCl) \tag{A28}$$

Since it is assumed that neutralization of a particular transport site eliminates the linebroadening due to that site but has no effect on other sites, the transport site linebroadening is given by

$$\delta = \delta(0)\,(1 - P_X) \tag{A29}$$

where $\delta(0)$ is the transport site linebroadening when high pH inhibition is negligible, and P_X is the fraction of transporters that have been inhibited by base titration.

Dependence of the Fractional Inhibition on pH. The fractional inhibition is simply the number of inhibited transporters divided by the total number of transporters, or

$$P_X = \frac{E_O + E_I}{E_O + E_OH + E_OHCl + E_I + E_IH + E_IHCl} \tag{A30}$$

This expression can be rewritten using the definitions of K_{D_O}, K_{D_I}, K_{A_O}, K_{A_I}, and Equation A28 as well as the condition $H_O = H_I = H$ to yield

$$P_X = \frac{H^{-1}}{H^{-1} + \overline{K_A}^{-1}} \tag{A31}$$

where the macroscopically observed quantity $\overline{K_A}$ is

$$\overline{K_A} = \frac{K_{A_O}\cdot\frac{K_{D_O}}{Cl_O}\cdot\frac{1}{k_{OI}} + K_{A_I}\cdot\frac{K_{D_I}}{Cl_I}\cdot\frac{1}{k_{IO}}}{\frac{1}{k_{OI}}\left(1 + \frac{K_{D_O}}{Cl_O}\right) + \frac{1}{k_{IO}}\left(1 + \frac{K_{D_I}}{Cl_I}\right)} \tag{A32}$$

This expression simplifies when the condition $Cl_O = Cl_I = Cl$ holds:

$$\overline{K_A} = \left(K_{A_O}\cdot\frac{K_{D_O}}{k_{OI}} + K_{A_I}\cdot\frac{K_{D_I}}{k_{IO}}\right)\Bigg/\left(\left(\frac{K_{D_O}}{k_{OI}} + \frac{K_{D_I}}{k_{IO}} + Cl\left(\frac{1}{k_{OI}} + \frac{1}{k_{IO}}\right)\right)\right) \tag{A33}$$

Inasmuch as we have derived Equation A33 assuming that chloride binding is a competitive inhibitor of deprotonation (see "Assumptions"), it is expected that $\overline{K_A}$ depends upon the chloride concentration; when the chloride concentration increases, deprotonation ($\overline{K_A}$) decreases accordingly.

In order to obtain the predicted form of the titration curve, Equation A31 can be reexpressed in terms of the pH and $\overline{pK_A}$ (= $-\log_{10}\overline{K_A}$):

$$P_X = \frac{10^{pH}}{10^{pH} + 10^{\overline{pK_A}}} \tag{A34}$$

This result can be substituted into Equation A29 to yield the pH-dependence of the linebroadening due to a ping-pong transporter:

$$\delta = \delta(0)\left(1 - \frac{10^{pH}}{10^{pH} + 10^{\overline{pK_A}}}\right) \tag{A35}$$

Thus, a ping-pong transporter has a simple base titration curve and a single macroscopically observed $\overline{pK_A}$.

APPENDIX II. THE pK_A FOR BASE TITRATION OF AN ANION BINDING SITE: EFFECT OF ANION CONCENTRATION

We estimate here the effect of an anion concentration on the pK_A of an essential positive charge in an anion binding site. It is assumed that the anion can only bind to the site when it is protonated and that deprotonation can only occur when the site is empty of anion; in other words, anion binding and deprotonation are mutually exclusive. It is this competition with anion binding that causes the pK_A for deprotonation to depend on the anion concentration. The final result is generalizable for any site for which anion binding and deprotonation are mutually exclusive.

For a ping-pong transporter the macroscopically observed quantity $\overline{pK_A}$ is given by (Appendix I)

$$\overline{pK_A} = \log_{10}\left[\frac{K_{D_O}\tau_{OI} + K_{D_I}\tau_{IO} + Cl(\tau_{OI} + \tau_{IO})}{K_{A_O}K_{D_O}\tau_{OI} + K_{A_I}K_{D_I}\tau_{IO}}\right] \tag{A36}$$

Unfortunately, at the present time the microscopic chloride and proton dissociation constants (K_{D_x} and K_{A_x}) and the inverse rate constants ($\tau_{xy} = 1/k_{xy}$) are all unknown for the band 3 ping-pong transport cycle. Thus, to proceed further, we must assume that $K_{D_O} = K_{D_I} = K_D$ and $K_{A_O} = K_{A_I} = K_A$ in order to simplify the expression. Doing so yields

$$\overline{pK_A} = \log_{10}\left[\frac{1}{K_A}\cdot\frac{K_D + Cl}{K_D}\right] \tag{A37}$$

This is simply the expression expected for any classical anion binding site for which deprotonation and anion binding are mutually exclusive. For the case of interest (see text, Figure 4) the site is the band 3 transport site, for which we will assume K_D = 80 mM (2), and the anion is 250 mM chloride. Use of these values yields an increase in $\overline{pK_A}$ of 0.6 units relative to the $\overline{pK_A}$ observed in the absence of chloride.